Guest water-induced reversible regulation of proton conduction in a two-dimensional nickel(II) coordination polymer

Ao-Na Sun, Fu-Wan Dong, Yi-Chen, Si-Chen Zhang, Rui-Han Liu, Junlun Zhu, and Dong Shao *

Hubei Key Laboratory of Processing and Application of Catalytic Materials, Hubei Provincial Engineering Research Center of High Purity Raw Material Processing Technology of Electronic Materials, College of Chemistry and Chemical Engineering, Huanggang Normal University, Huanggang 438000, China

Correspondence and requests for materials should be addressed to

Email: shaodong@nju.edu.cn

Table of Contents

EXPERIMENTAL SECTION

Physical measurements

Elemental analyses of C, H, and N were performed at an Elementar Vario MICRO analyzer. Infrared spectra were obtained in the range of 500–4000 cm^{-1} on a Bruker tensor II spectrometer. Powder X-ray diffraction data (PXRD) were recorded on a Bruker D8 Advance diffractometer with Cu Kα X-ray source (λ = 1.54056 Å) operated at 40 kV and 40 mA between 5 and 30° (2θ). Thermal gravimetric analysis (TGA) was carried out on freshly filtered crystals using the Mettler Toledo TGA2 instrument in an insert Ar atmosphere over a temperature range of 27–700 °C with a heating rate of 10 °C/min. Water adsorption/desorption isotherms were measured using a BELSORP max instrument.

X-ray Crystallography

Single crystal X-ray diffraction data were collected on a Bruker D8 QUEST diffractometer with a PHOTON III area detector (Mo-Kα radiation, λ = 0.71073 Å, Bruker *IuS* 3.0) at different temperatures controlled by Oxford Cryosystems low-temperature device. The APEX III program was used to determine the unit cell parameters and for data collection. The data were integrated and corrected for Lorentz and polarization effects using SAINT.[S1] Absorption corrections were applied with SADABS.[S2] The structures were solved by direct methods and refined by full-matrix least-squares method on F^2 using the SHELXTL[S3] crystallographic software package integrated in Olex2.[S4] All the non-hydrogen atoms were refined anisotropically. Hydrogen atoms of the organic ligands were refined as riding on the corresponding non-hydrogen atoms. Additional details of the data collections and structural refinement parameters are provided in Table 1. Selected bond lengths and angles are listed in Table S1, S2. CCDC numbers 2491444 (**Ni**·$6H_2O$), 2491445 (**Ni**·$2H_2O$), 2491446 (**Ni**·$6H_2O$_re) are the supplementary crystallographic data for this paper. They

can be obtained freely from the Cambridge Crystallographic Data Centre via www.ccdc.cam.ac.uk/data_request/cif.

Proton conductivity

Alternating current (AC) impedance measurements were performed for a pellet attached to an Au paste with a gold conducting wire using an electrochemical workstation (DH7007). The test cells containing the pellets were suspended in a commercial temperature and humidity control chamber (DHTHM-27-0-P-SD). Data were collected in steps of 10 °C in a frequency range of 0.1 Hz to 1 MHz and an AC amplitude of 100 mV, thermally equilibrated for 1 h at each temperature. Bulk conductivities were estimated by a semicircle fitting of Nyquist plots. Proton conductivity (σ) is estimated by the following equation,

$$\sigma = L / A \cdot R \quad (1),$$

where L and A are the thickness and area of the pellet and R is the bulk resistance estimated by the Nyquist plot. Activation energy of proton conduction (Ea) is estimated by the following equation,

$$\sigma T = \sigma_0 \exp\left(E_a / kBT\right) \quad (2),$$

where σ is the proton conductivity, σ_0 is the preexponential factor, k_B is the Boltzmann constant, and T is the temperature.

Table S1. Selected bond lengths (Å) in **Ni**·6H_2O.

Parameter	bond lengths (Å)	Parameter	bond lengths
Ni1-O1	2.118(2)	Ni2-O1	2.096(2)
Ni1-O8	2.108(2)	Ni2-O5	2.089(2)
Ni1-O14	2.092(2)	Ni2-O6	2.126(2)
Ni1-O16	2.036(2)	Ni2-O20	2.053(2)
Ni1-N1	2.065(2)	Ni2-N2$^{\#}$	2.076(2)
Ni1-N3*	2.083(2)	Ni2-N4	2.053(2)

*1-X,1/2+Y,3/2-Z; $^{\#}$-X,-1/2+Y,1/2-Z

Table S2. Selected bond angles (°) in **Ni**·6H_2O.

Parameter	bond angles
O8-Ni1-O4	88.63(7)
O14-Ni1-O4	88.86(7)
O14-Ni1-O8	173.52(6)
O16-Ni1-N1	171.26(7)
O16-Ni1-N3*	90.15(8)
N1-Ni1-N3*	96.48(8)
O1-Ni2-O6	87.80(8)
O5-Ni2-O1	90.80(7)
O5-Ni2-O6	173.15(6)
O20-Ni2-N4	171.40(7)
N4-Ni2-O5	91.48(8)
N4-Ni2-O6	91.48(8)
N4-Ni2-N2$^{\#}$	93.51(7)

*1-X,1/2+Y,3/2-Z; $^{\#}$-X,-1/2+Y,1/2-Z

Table S3. Selected bond lengths (Å) in **Ni**·2H_2O.

Parameter	bond lengths (Å)	Parameter	bond lengths (Å)
Ni1-O1	2.083(11)	Ni2-O1	2.111(10)
Ni1-O4	2.040(8)	Ni2-O5	2.051(9)
Ni1-O5	2.097(10)	Ni2-O6	2.083(10)
Ni1-O7	2.095(10)	Ni2-O20	2.123(13)
Ni1-N1	2.111(15)	Ni2-N1*	2.061(17)
Ni1-N2	2.048(12)	Ni2-N4#	2.090(11)

*1-X,1/2+Y,3/2-Z; #-X,-1/2+Y,1/2-Z

Table S4. Selected bond angles (°) in **Ni**·2H_2O.

Parameter	bond angles
O1-Ni1-O5	89.3(4)
O1-Ni1-O7	89.5(4)
O1-Ni1-N1	174.6(5)
O4-Ni1-N2	171.3(5)
O5-Ni1-N1	93.7(5)
O7-Ni1-N5	172.9(4)
O6-Ni2-O11	172.6(4)
O8-Ni2-N3*	89.6(6)
O8-Ni2-N4#	173.3(5)
N3*-Ni2-O6	92.0(5)
N3*-Ni2-O10	174.5(6)
C4-N2-Ni2	122.2(12)
C30-O4-Ni1	130.8(10)

*1-X,1/2+Y,3/2-Z; #-X,-1/2+Y,1/2-Z

Table S5. Continuous Shape Measure (CShM) analysis for six-coordinated Ni(II) in **Ni**·6H_2O and **Ni**·2H_2O.

Compound,	Metal center	CSM parameters* six-coordinated coordination sphere					Determined coordination geometry
		HP-6	PPY-6	OC-6	TPR-6	JPPY-6	
Ni·6H_2O	Ni1	32.361	27.237	**0.290**	15.055	31.236	OC-6
	Ni2	32.646	26.774	**0.349**	14.472	30.663	OC-6
Ni·2H_2O	Ni1	32.566	27.318	**0.316**	14.918	31.261	OC-6
	Ni2	31.477	27.310	**0.308**	15.162	31.370	OC-6

*CShM parameters for six-coordinated complexes:

HP-6 - the parameter related to the hexagon (D_{6h});

PPY-6 - the parameter related to the pentagonal pyramid (C_{5v});

OC-6 - the parameter related to the octahedron (O_h);

TPR-6 - the parameter related to the trigonal prism (D_{3h});

JPPY-6 - the parameter related to the Johnson pentagonal pyramid (*C5v*)

Table S6. The possible hydrogen bonds in **Ni**·6H_2O calculated by PLATON.

D-H...Acceptor	d(D-	d(H...A)	d(D...A)	＜(DHA)
O(1)-H(1A)...O(3)[1]	0.87	1.84	2.706(3)	172
O(1)-H(1B)...O(12)	0.87	1.94	2.803(3)	174
O(2)-H(2A)...O(17)	0.87	2.00	2.861(4)	173
O(2)-H(2B)...O(9)	0.87	2.06	2.926(5)	176
O(4)-H(4A)...O(18)	0.87	2.04	2.912(3)	174
O(4)-H(4B)...O(13)[2]	0.87	1.83	2.696(3)	172
O(5)-H(5A)...O(12)[1]	0.87	1.82	2.692(2)	176
O(5)-H(5B)...O(3)	0.87	2.26	3.100(3)	162
O(6)-H(5A)...O(10)3	0.87	1.88	2.744(3)	170
O(6)-H(5B)...O(10)	0.87	1.98	2.750(3)	147
O(7)-H(5A)...O(10)	0.87	2.09	2.950(3)	171
O(7)-H(5B)...O(10)	0.87	2.00	2.840(3)	160
O(8)-H(8A)...O(11)[4]	0.87	1.85	2.717(3)	173
O(8)-H(8B)...O(11)	0.87	1.98	2.742(3)	146
O(9)-H(5A)...O(10)	0.87	1.88	2.717(4)	160
O(14)-H(14A)...O(18)[2]	0.87	2.23	2.714(2)	167
O(14)-H(14B)...O(13)	0.87	2.21	3.080(3)	161
O(15)-H(15A)...O(6)[5]	0.87	1.94	3.041(3)	174
O(15)-H(15B)...O(12)[6]	0.87	2.06	2.807(3)	159
O(17)-H(17D)...O(15)	0.87	2.26	2.889(4)	154
O(19)-H(19A)...O(15)	0.87	2.29	3.063(5)	165
O(19)-H(19B)...O(9)	0.87	2.29	3.145(5)	174

Symop-for-A:

[1]1-X,1-Y,1-Z; [2]-X,-Y,1-Z; [3]-X,1-Y,1-Z; [4]1-X,-Y,1-Z; [5]-X,-1/2+Y,1/2-Z; [6]+X,1/2-Y,-1/2+Z

Table S7. The possible hydrogen bonds in **Ni**·2H_2O calculated by PLATON.

D-H...Acceptor	d(D-	d(H...A)	d(D...A)	＜(DHA)
O(1)-H(1A)...O(13)[1]	0.87	1.97	2.734(13)	147
O(1)-H(1B)...O(14)	0.87	2.06	2.839(14)	150
O(5)-H(5A)...O(2)1	0.87	1.86	2.675(13)	155
O(5)-H(5B)...O(9)	0.87	2.30	3.156(17)	170
O(6)-H(6A)...O(14)2	0.86	1.86	2.719(14)	174
O(6)-H(6B)...O(13)	0.86	2.26	3.104(16)	167
O(7)-H(7A)...O(12)3	0.87	1.91	2.760(17)	168
O(7)-H(7B)...O(3)	0.87	1.95	2.724(14)	148
O(10)-H(10A)...O(9)[2]	0.92	1.82	2.674(14)	173
O(10)-H(10B)...O(2)	0.85	2.04	2.885(13)	168
O(11)-H(11A)...O(12)	0.85	1.86	2.738(14)	160
O(11)-H(11B)...O(3)[4]	0.85	1.86	2.763(19)	160
O(16)-H(16A)...O(7)	0.85	2.22	3.06(3)	168
O(16)-H(16B)...O(2)3	0.85	2.03	2.85(3)	164
O(18)-H(18A)...O(19)	0.85	1.97	2.79(7)	163
O(18)-H(18B)...O(17)	0.85	1.97	2.84(19)	163
O(19)-H(19A)...O(11)[6]	0.85	2.37	3.21(6)	171
O(19)-H(19B)...O(14)[8]	0.85	2.60	2.99(5)	167

Symop-for-A:
[1]-1/2+X,-1/2+Y,+Z; [2]1/2+X,1/2+Y,+Z; [3]1/2+X,-1/2+Y,+Z; [4]-1/2+X,1/2+Y,+Z; [5]+X,1-Y,1/2+Z; [6]1+X,1-Y,1/2+Z; [7]+X,-1+Y,+Z; [8]1/2+X,1/2-Y,1/2+Z

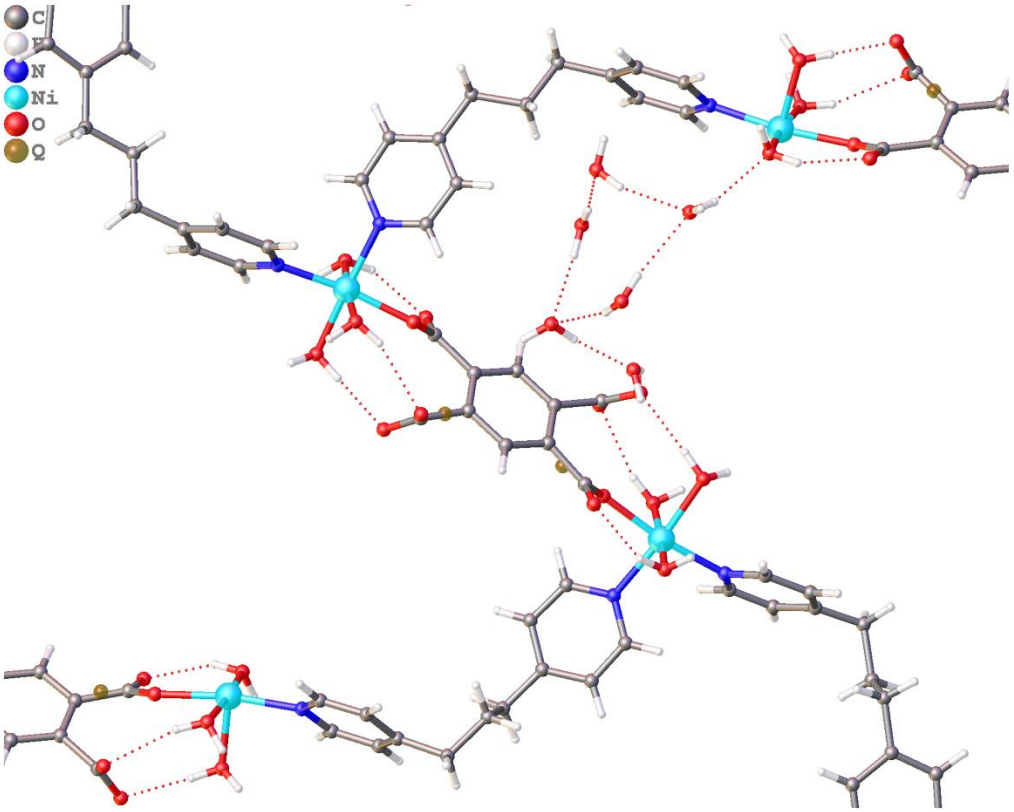

Figure S1. The structure of **Ni**·6H_2O by growing operation.

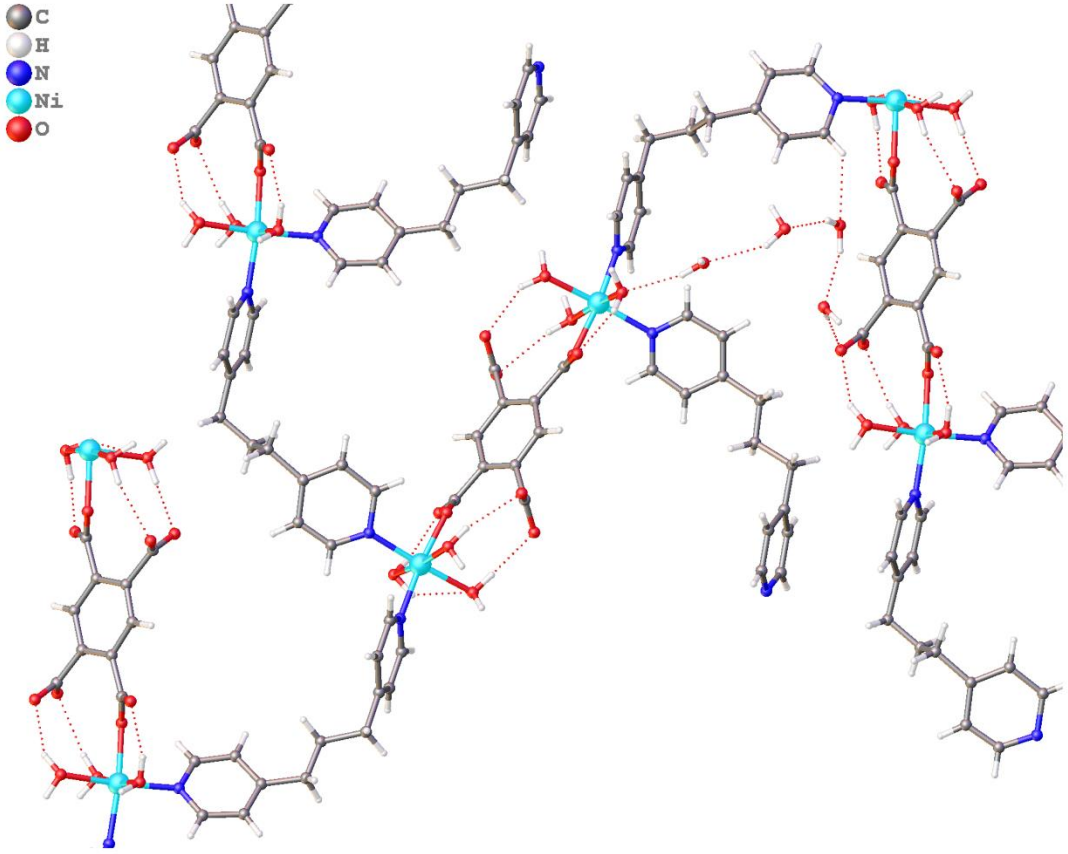

Figure S2. The structure of **Ni**·2H_2O by growing operation.

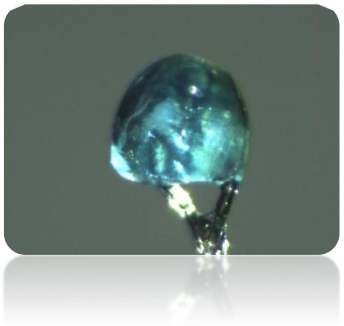

Figure S3. The optical images of single crystals of **Ni**·6H_2O_re.

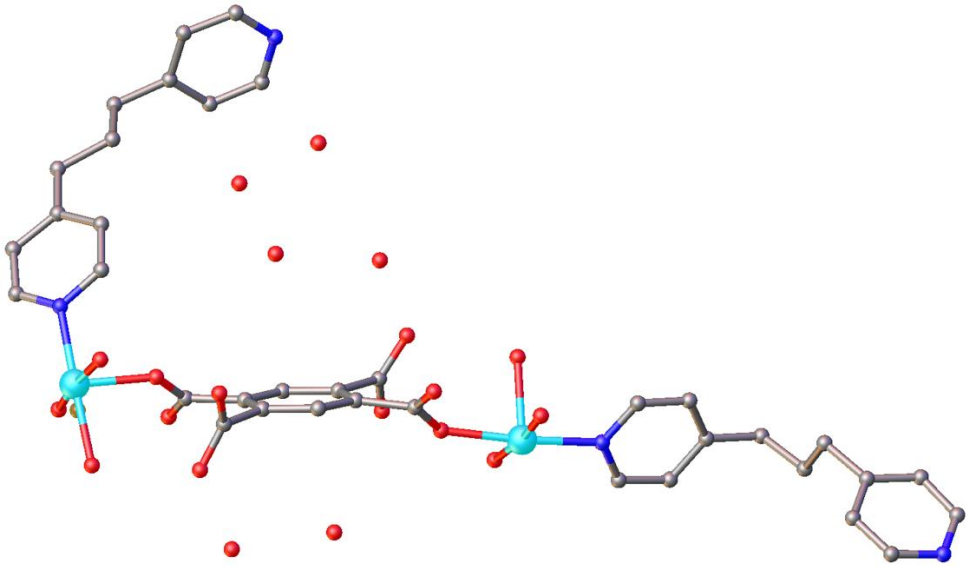

Figure S4. The asymmetric unit of rehydrated phase **Ni**·6H_2O_re.

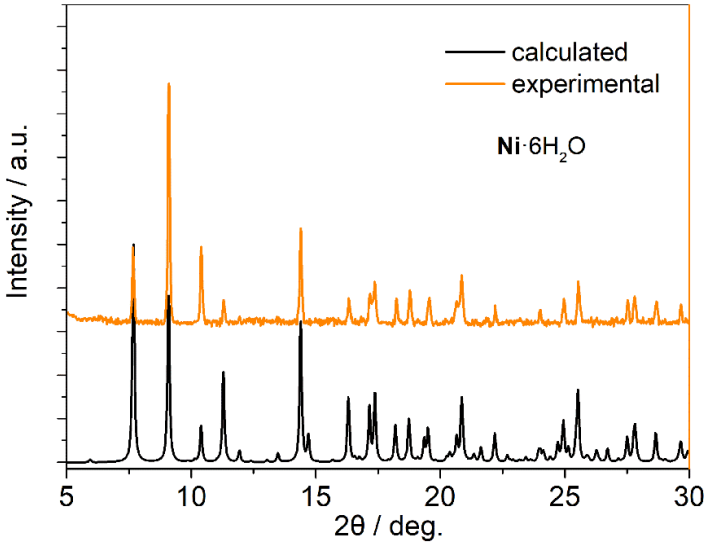

Figure S5. PXRD pattern for **Ni**·$6H_2O$.

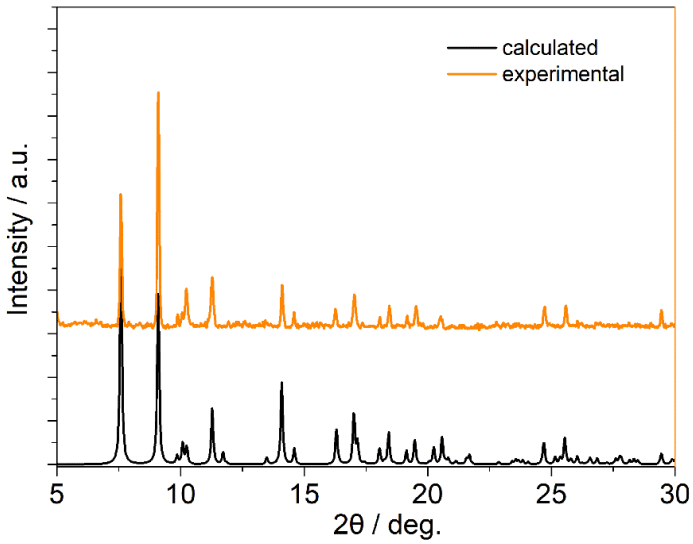

Figure S6. PXRD pattern for **Ni**·$2H_2O$.

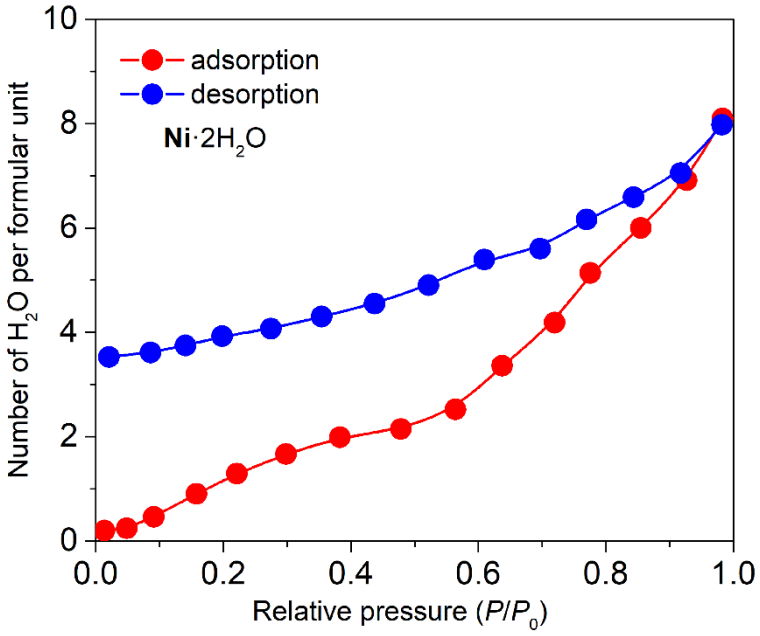

Figure S7. H_2O adsorption isotherms of **Ni**·$2H_2O$ under different RH at 25 °C.

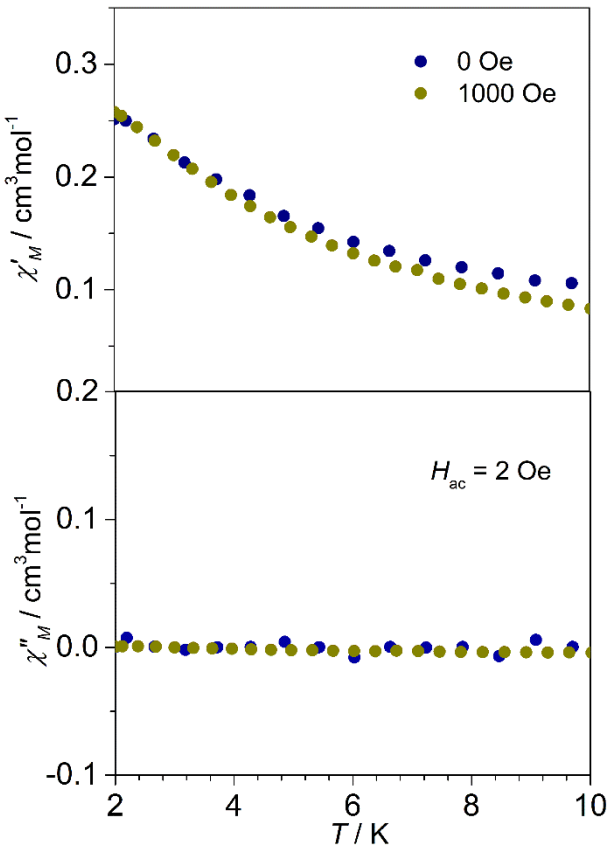

Figure S8. Temperature dependence of the in-phase (χ') and out-of-phase (χ'') part of the ac susceptibilities measured under zero dc field for **Ni**·6H_2O.

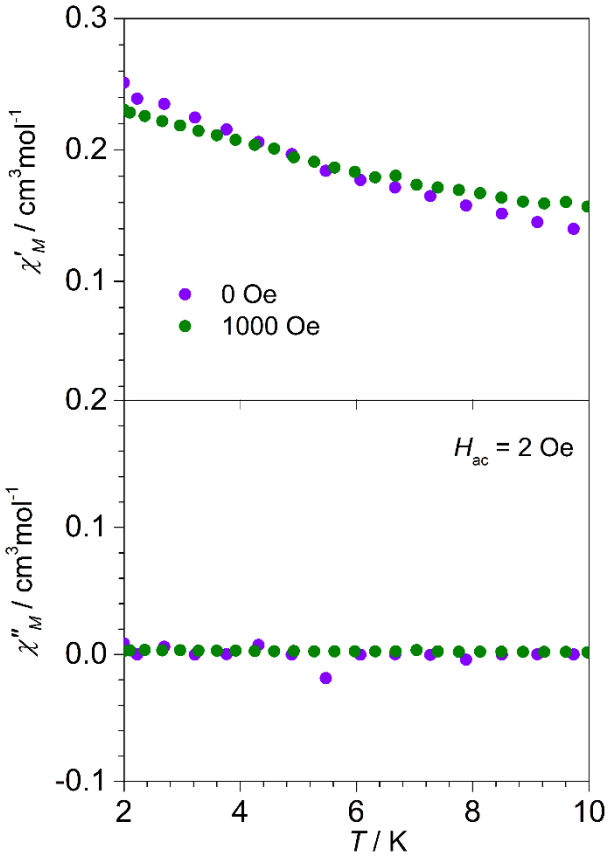

Figure S9. Temperature dependence of the in-phase (χ') and out-of-phase (χ'') part of the ac susceptibilities measured under zero dc field for **Ni**·2H_2O.

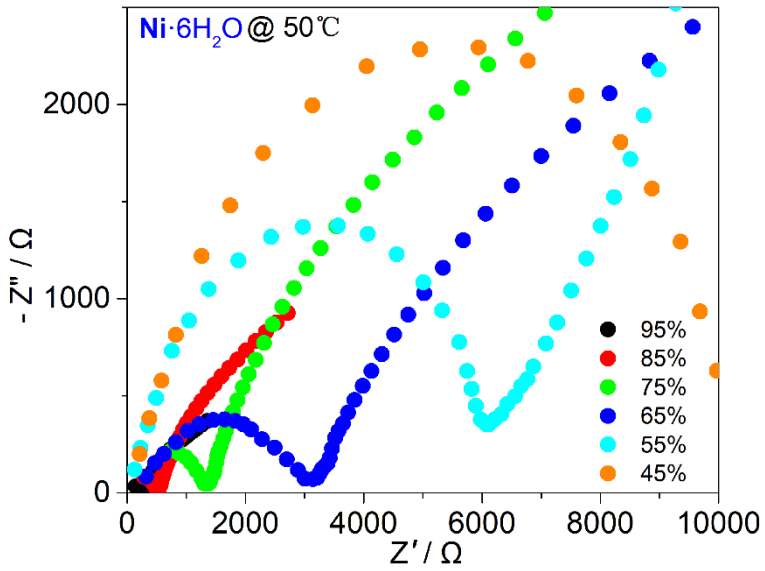

Figure S10. Humidity dependence of conductivity at 50 °C of **Ni**·6H_2O.

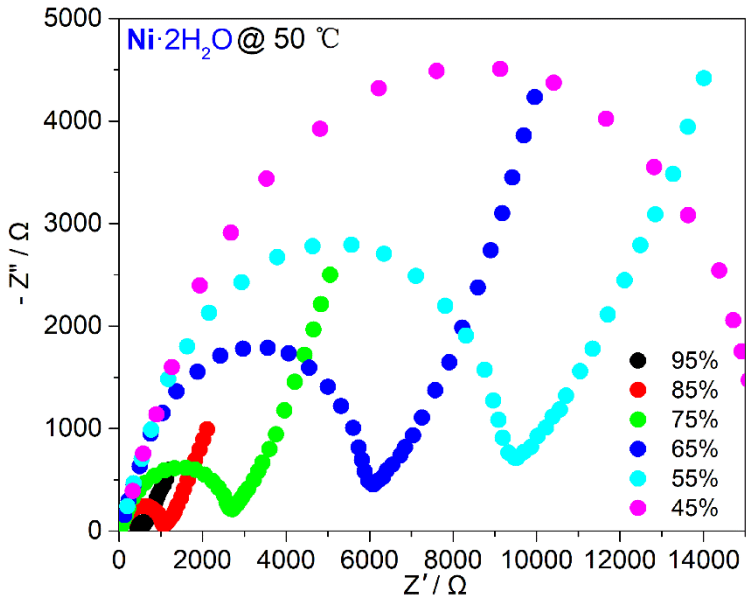

Figure S11. Humidity dependence of conductivity at 50 °C of **Ni**·2H$_2$O.

Table S8. The conductivity of **Ni**·6H_2O extracted from impedance spectra gathered at 50 °C under variable indicated relative humidity.

RH%	σ / S cm^{-1}
45	2.7×10^{-5}
55	4.9×10^{-5}
65	7.2×10^{-5}
75	9.3×10^{-5}
85	2.2×10^{-4}
95	4.7×10^{-4}

Table S9. The conductivity of **Ni**·2H_2O extracted from impedance spectra gathered at 50 °C under variable indicated relative humidity.

RH%	σ / S cm^{-1}
45	4.7×10^{-7}
55	1.9×10^{-6}
65	4.2×10^{-6}
75	7.8×10^{-5}
85	3.1×10^{-4}
95	4.1×10^{-4}

Table S10. The conductivity of **Ni**·6H_2O extracted from impedance spectra gathered at different temperature under 95% relative humidity.

T / °C	σ / S cm^{-1}
30	1.1×10^{-5}
35	3.1×10^{-5}
40	5.5×10^{-5}
45	8.3×10^{-5}
50	2.8×10^{-4}
55	3.3×10^{-4}
60	4.6×10^{-4}

Table S11. The conductivity of **Ni**·2H_2O extracted from impedance spectra gathered at different temperature under 45% relative humidity.

T / °C	σ / S cm^{-1}
30	1.1×10^{-7}
40	2.2×10^{-7}
50	4.8×10^{-7}
60	6.0×10^{-7}
70	8.1×10^{-7}
80	9.3×10^{-7}
90	1.2×10^{-6}

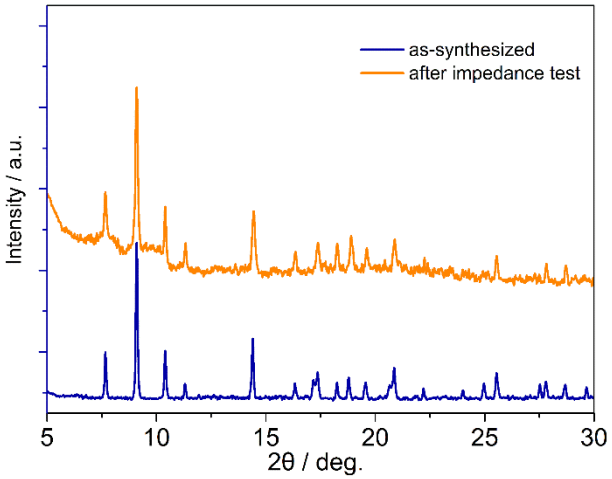

Figure S12. PXRD pattern after impedance measurements for **Ni**·$6H_2O$.

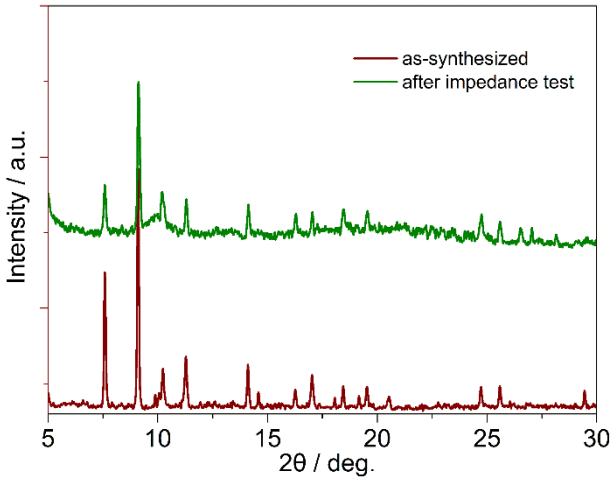

Figure S13. PXRD pattern after impedance measurements for **Ni**·$2H_2O$.

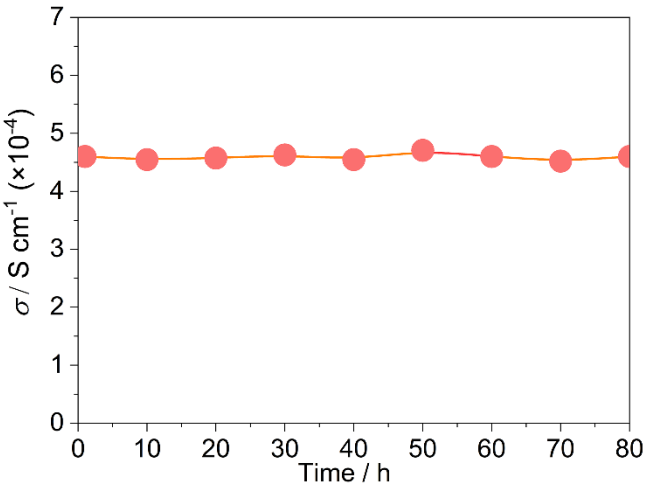

Figure S14. Time-dependent proton conductivity of **Ni**·6H_2O at 60 °C and 95% RH.

References

S1) SAINT Software Users Guide, version 7.0; Bruker Analytical X-Ray Systems: Madison, WI, 1999.

S2) G. M. Sheldrick, SADABS, version 2.03; Bruker Analytical X-Ray Systems, Madison, WI, 2000.

S3) G. M. Sheldrick, SHELXTL, Version 6.14, Bruker AXS, Inc.; Madison, WI 2000-2003.

S4) O. V. Dolomanov, L. J. Bourhis, R. J. Gildea, J. A. K. Howard, H. Puschmann, OLEX2: A Complete Structure Solution, Refinement and Analysis Program. *J. Appl. Crystallogr*., 2009, 42, 339−341.